PHILOSOPHICAL TRANSACTIONS OF THE ROYAL SOCIETY B

Phil. Trans. R. Soc. B (2012) **367**, 1047–1058
doi:10.1098/rstb.2011.0203

Review

Structure and mechanism of the tripartite CusCBA heavy-metal efflux complex

Feng Long[1], Chih-Chia Su[1], Hsiang-Ting Lei[1], Jani Reddy Bolla[1], Sylvia V. Do[2] and Edward W. Yu[1,2,3,*]

[1]*Department of Chemistry,* [2]*Bioinformatics and Computational Biology Interdepartmental Graduate Program, and* [3]*Department of Physics and Astronomy, Iowa State University, Ames, IA 50011, USA*

Gram-negative bacteria frequently expel toxic chemicals through tripartite efflux pumps that span both the inner and outer membranes. The three parts are the inner membrane, substrate-binding transporter (or pump); a periplasmic membrane fusion protein (MFP, or adaptor); and an outer membrane-anchored channel. The fusion protein connects the transporter to the channel within the periplasmic space. One such efflux system CusCBA is responsible for extruding biocidal Cu(I) and Ag(I) ions. We previously described the crystal structures of both the inner membrane transporter CusA and the MFP CusB of *Escherichia coli*. We also determined the co-crystal structure of the CusBA adaptor–transporter efflux complex, showing that the transporter CusA, which is present as a trimer, interacts with six CusB protomers and that the periplasmic domain of CusA is involved in these interactions. Here, we summarize the structural information of these efflux proteins, and present the accumulated evidence that this efflux system uses methionine residues to bind and export Cu(I) and Ag(I). Genetic and structural analyses suggest that the CusA pump is capable of picking up the metal ions from both the periplasm and the cytoplasm. We propose a stepwise shuttle mechanism for this pump to export metal ions from the cell.

Keywords: tripartite efflux pump; multidrug resistance; resistance-nodulation-cell division; heavy-metal efflux; CusCBA; X-ray crystallography

1. INTRODUCTION

Silver is a heavy metal with a relatively high toxicity in prokaryotes. Ionic silver exhibits antimicrobial activity against a broad range of micro-organisms, and has long been used as an effective broad antimicrobial agent against pathogens [1,2]. Copper, although required in trace amounts for bacterial growth, is highly toxic even at low concentrations [3]. Thus, both silver and copper are well-known bactericides, and their biocidal effects have been used for centuries. In Gram-negative bacteria, efflux systems of the resistance-nodulation-cell division (RND) superfamily play major roles in the intrinsic and acquired tolerance of antibiotics and toxic compounds, including silver and copper ions [4,5]. The Gram-negative bacterium *Escherichia coli* harbours seven different RND efflux transporters. These seven transporters can be categorized into two distinct subfamilies, the hydrophobic and amphiphilic efflux RND (HAE-RND) and heavy-metal efflux RND (HME-RND) families [4,5]. Six of these transporters, such as AcrB [6–16], AcrD [7,17,18], AcrF [7,19,20], MdtB [7,21,22], MdtC [7,21,22] and YhiV [7,23,24], are multidrug efflux pumps, which belong to the HAE-RND protein family [4]. In addition to these multidrug efflux pumps, *E. coli* contains one HME-RND efflux transporter, CusA, which specifically recognizes and confers resistance to Ag(I) and Cu(I) ions [25,26].

As an RND transporter, CusA works in conjunction with a periplasmic component, belonging to the membrane fusion protein (MFP) family, and an outer membrane channel (OMC) to form a functional protein complex. CusA is a large proton motive force-dependent inner membrane efflux pump comprising 1047 amino acids [25,26]. CusC, however, is a 457 amino acid protein that forms an OMC [25,26]. The MFP CusB (379 amino acids) contacts both the inner membrane CusA and outer membrane CusC proteins [25,26]. Presumably, the three components of this HME-RND system form a tripartite efflux complex CusCBA, which spans both the inner and outer membranes of *E. coli* to export Ag(I) and Cu(I) directly out of the cell. Heavy-metal efflux by the CusCBA complex is driven by proton import, and this process is catalysed through the inner membrane transporter CusA.

Between the *cusC* and *cusB* genes, there is a small chromosomal gene that produces a periplasmic protein CusF [26]. CusF is also involved in Cu(I)/Ag(I) resistance. It functions as a chaperone that carries Cu(I)/Ag(I) to the CusCBA tripartite efflux pump [27,28].

Among those transporters belonging to the RND superfamily, the structural and functional relationships of the HAE-RND pumps have been elucidated extensively. Currently, two crystal structures of the

* Author for correspondence (ewyu@iastate.edu).

One contribution of 11 to a Theme Issue 'Bacterial protein secretion comes of age'.

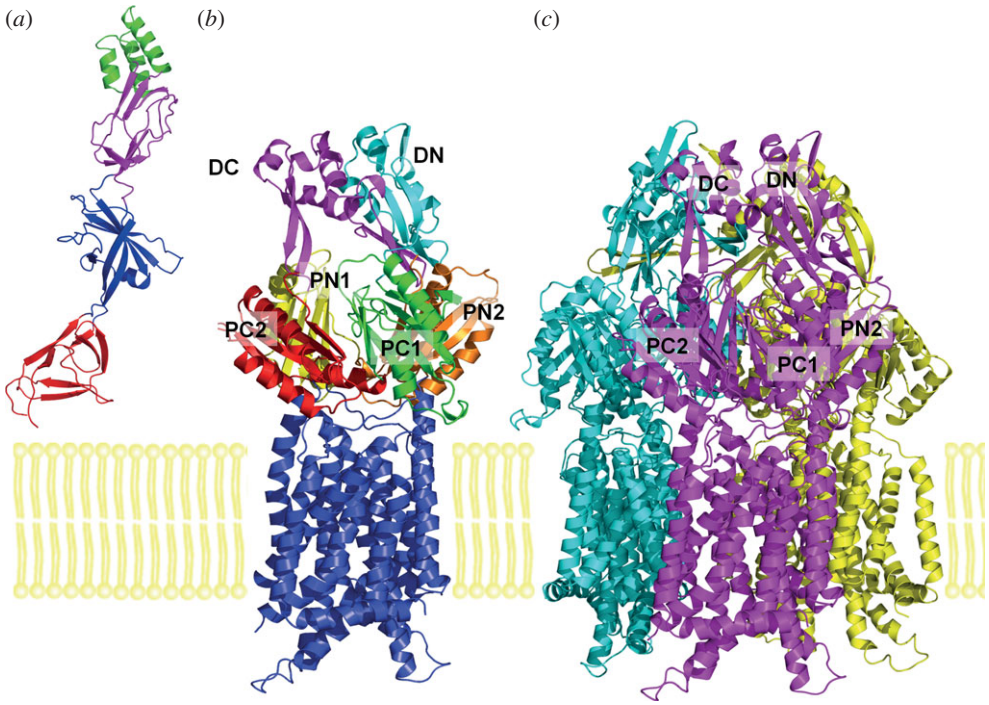

Figure 1. Crystal structures of the CusB and CusA efflux proteins. (*a*) Ribbon diagram of the CusB protomer. The structure can be divided into four distinct domains. Domain 1 (red) is formed by the N- and C-termini and is located above the inner membrane. The loops between domains 2 (blue) and 3 (magenta) appear to form an effective hinge to allow the molecule to shift from an open conformation to a more compact structure. Domain 4 (green) is folded into an anti-parallel, three-helix bundle, which is thought to be located near the outer membrane. (*b*) Ribbon diagram of the CusA protomer viewed in the membrane plane. Sub-domains DN, DC, PN1, PN2, PC1 and PC2 are coloured cyan, magenta, yellow, orange, green and red, respectively. The transmembrane helices are coloured blue. (*c*) Ribbon diagram of the CusA homotrimer viewed in the membrane plane. Each subunit of CusA is labelled with a different colour. Sub-domains DN, DC, PN2, PC1 and PC2 are labelled on the front protomer (magenta). The location of PN1 in this protomer is behind PN2, PC1 and PC2 (see text).

HAE-RND-type efflux pumps, the *E. coli* AcrB [8–16] and *Pseudomonas aeruginosa* MexB [29] multidrug transporters, have been determined. Their structures suggest that both AcrB and MexB span the entire width of the inner membrane and protrude approximately 70 Å into the periplasm. Along with the models of these two HAE-RND transporters, the crystal structures of the other components of these tripartite complex systems have also been determined. These include the OMCs *E. coli* TolC [30] and *P. aeruginosa* OprM [31], as well as the periplasmic MFPs *E. coli* AcrA [32] and *P. aeruginosa* MexA [33–35].

Different from the HAE-RND family, members of the HME-RND family are highly substrate-specific, with the ability to differentiate between monovalent and divalent ions. To elucidate the mechanism used by the CusCBA efflux system for Cu(I)/Ag(I) recognition and extrusion, we recently determined the crystal structures of the CusB MFP [36] and the CusA inner membrane efflux pump [37], both in the absence and presence of Cu(I) or Ag(I). We also described the co-crystal structure of the CusBA adaptor–transporter complex [38]. The structure indicates that the complete assembly of the CusCBA tripartite efflux complex should be in the form of $CusC_3$–$CusB_6$–$CusA_3$ that spans both the inner and outer membranes of *E. coli* and extrudes Cu(I) and Ag(I) ions [38]. In this review, we summarize the structural information on these efflux proteins. Based on the new findings about this efflux system, we put forward our opinion on how these protein machines facilitate metal transport. The structures strongly suggest that the CusCBA efflux system relies upon methionine residues to bind and export the metal ions.

2. CRYSTAL STRUCTURE OF THE CusB MEMBRANE FUSION PROTEIN

The crystal structure of CusB (pdb code: 3H9I), comprising approximately 80 per cent of the protein (residues 89–385), was originally determined to a resolution of 3.40 Å [36]. The structure revealed that the asymmetric unit of the crystal consists of two protomers. These two CusB molecules were found to interact with each other. Each CusB molecule is folded into an elongated polypeptide approximately 120 Å long and 40 Å wide. Intriguingly, this adaptor protein can be divided into four different domains (figure 1*a*). The first three domains of the protein are mostly β-strands. However, the fourth domain forms an all α-helical domain, which is folded into a three-helix bundle secondary structure.

The first β-domain (domain 1) of CusB is formed by the N- and C-terminal ends of the polypeptide (residues 89–102 and 324–385). This domain is located directly above the outer-leaflet of the inner membrane. Using lysine–lysine cross-linking coupled with liquid chromatography–tandem mass spectrometry (LC-MS/MS), it has been found that this domain specifically interacts with the periplasmic domain of the CusA efflux

pump [36]. Overall, domain 1 is a β-barrel domain, consisting of six β-strands, with the N-terminal end forming one of the β-strands while the C-terminus of the protein constitutes the remaining five strands (figure 1*a*).

The second β-domain (domain 2) of CusB is formed by residues 105–115 and 243–320. This domain comprises six β-strands and one short α-helix. Again, the N-terminal residues form one of the β-strands that is incorporated into this domain. The C-terminal residues contribute a β-strand, an α-helix and four anti-parallel β-sheets.

Domain 3 is another globular β-domain adjacent to the second domain of CusB. This domain consists of residues 121–154 and 207–239, with a majority of these residues folding into eight β-strands.

Perhaps, the most interesting motif appears to be in the fourth domain (domain 4) of CusB. This region, comprising residues 156–205, forms an all-helical domain. Surprisingly, this domain is folded into an anti-parallel, three-helix bundle [36]. This structural feature, not found in other known protein structures in the MFP family, highlights the uniqueness of the CusB protein. The helix bundle creates an approximately 27 Å long helix-turn-helix-turn-helix secondary structure, making it at least 20 Å shorter than the two-helical hairpin domains of MexA [33–35] and AcrA [32]. To date, CusB is the only periplasmic protein in the MFP family that possesses this three-helical domain instead of a two-helical hairpin motif.

The crystal structure of CusB represents the first structure of any MFP that is associated with an HME-RND-type transporter. Among all known structures of the MFP family, including AcrA [32] and MacA [39], the CusB [36], MexA [35] and most recently determined ZneB [40] proteins exhibit the most complete three-dimensional structures. Like MexA and ZneB, the structure of CusB revealed that this MFP consists of four major domains, including three β-strand domains and one α-helical domain. However, CusB is folded into a distinct secondary structure when compared with the other available MFP structures. This distinct structural feature may underscore the unique functionality of CusB in the MFP family.

There is strong evidence that members of the MFP family play a functional role in the efflux of substrates. It has been found that the MFP EmrA is able to directly bind different transported drugs [41]. Recently, it has also been shown that the CusB [42] and ZneB [40] proteins directly interact with the metal ions. Thus, it is expected that in addition to their role as adaptors to bridge the inner and outer membrane efflux components, these MFPs may participate in recognizing and extruding their substrates.

3. CRYSTAL STRUCTURE OF THE CusA HEAVY-METAL EFFLUX PUMP

The crystal structure of the CusA efflux pump [37] was resolved to a resolution of 3.52 Å, with 98 per cent of the residues (residues 5–504 and 516–1040) included in the final model (pdb code: 3KO7; figure 1*b*). Overall, the crystal structure of CusA is quite distinct from those of the HAE-RND pumps AcrB and MexB. Superimposition of the structure of CusA with the structure of AcrB results in a high r.m.s.d. of 11.4 Å for 1003 C^{α} atoms, suggesting highly significant differences between these two transporters. Sequence alignment shows that CusA and AcrB have only 19 per cent identity; thus it is not surprising that their secondary structures are distinct from each other. CusA exists as a homotrimer, and each subunit of CusA consists of 12 transmembrane helices (TM1–TM12) and a large periplasmic domain formed by two periplasmic loops between TM1 and TM2, and TM7 and TM8, respectively (figure 1*c*). In the transmembrane region, the relative locations of TM1–TM6 are related to those of TM7–TM12 by pseudo-twofold symmetry. These TM helices are arranged in such a way that TM4 and TM10 form the centre of the core and are surrounded by the other TM helices. Different from AcrB and MexB, four helices—TM4, TM5, TM10 and TM11—extend into the cytoplasm, forming the cytoplasmic domain of the pump. Two other helices, TM2 and TM8, protrude into the periplasm and contribute part of the periplasmic domain. It is important to note that TM2, TM4 and TM5 of the N-terminal half correspond to TM8, TM10 and TM11 of the C-terminal half, respectively, in the pseudo-twofold symmetry.

Like AcrB and MexB, the periplasmic domain of CusA can be divided into six sub-domains: PN1, PN2, PC1, PC2, DN and DC (figure 1*b*). Sub-domains PN1, PN2, PC1 and PC2 form the pore domain, with PN1 making up the central pore and stabilizing the trimeric organization. Sub-domains DN and DC, however, contribute to form the docking domain, presumed to be interacting with the OMC CusC. The trimeric CusA structure suggests that sub-domains PN2, PC1 and PC2 are located at the outermost core of the periplasmic domain, facing the periplasm. In AcrB, sub-domains PC1 and PC2 form a large external cleft and are presumed to create the entrance for drugs from the periplasm. However, the apo-CusA structure shows that the gap between PC1 and PC2 is completely closed (figure 1*c*). *In vitro* cross-linking coupled with mass spectrometry has suggested that sub-domain PN2 of CusA should interact with the N-terminus of the MFP CusB [36]. Thus, sub-domains PN2 and PC1 of CusA most likely form the binding surface for CusB.

Perhaps the most interesting secondary structural feature appears in the cleft region of the periplasmic domain. In figure 2, the residues located on the left wall, formed by one α-helix (residues 690–706) and three β-sheets (residues 681–687, 711–716 and 821–827), appear to tilt into the cleft to close the opening. Surprisingly, residues 665–675, located at the bottom of the cleft, form an α-helix. This structural feature, not found in AcrB and MexB, likely governs the specificity of the CusA pump. The α-helix orients horizontally and roughly divides the transmembrane and periplasmic domains into two compartments. Located just above this horizontal helix, we find three proximal methionine residues, M573, M623 and M672, presumably creating a three-methionine specific binding site for Cu(I) and Ag(I) ions [43,44]. Notably, M672 is also one of the residues within the horizontal helix. Site-directed mutagenesis had suggested that these three-methionine residues are essential for mediating copper resistance [26].

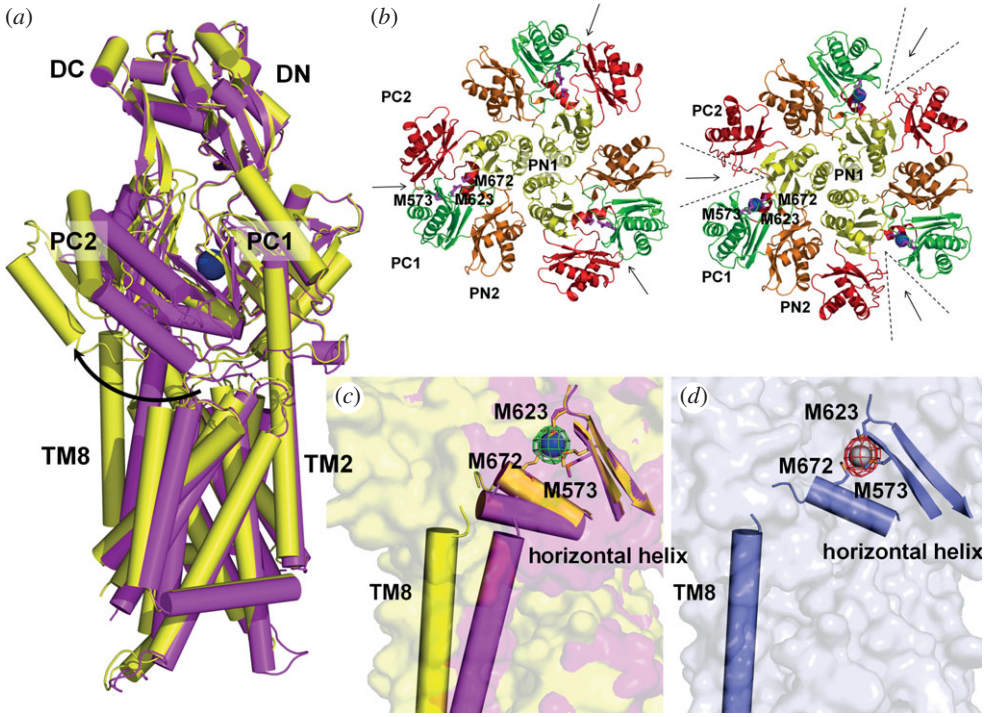

Figure 2. Comparison of the apo and metal bound structures of CusA. (*a*) Superimposition of a monomer of apo-CusA (magenta) onto a monomer of Cu(I) bound-CusA (yellow). The bound Cu(I) is in blue. The arrow represents a major swing of the PC2 sub-domain initiated by Cu(I) binding. (*b*) Conformational changes of the periplasmic domain of CusA. The conformation of each sub-domain of CusA before (left) and after (right) Cu(I) binding. The periplasmic cleft formed between PC1 and PC2 is opened after Cu(I) binding. The bound coppers in the CusA–Cu(I) structure are coloured blue. M573, M623 and M672 forming a metal binding site at the periplasmic cleft are shown in stick form (magenta). (*c*) The changes in conformation of the horizontal helix and TM8, are shown in a superimposition of the structures of apo (magenta) and Cu(I)-bound (yellow) CusA. The bound Cu(I) is shown as a blue sphere. Anomalous map of the bound Cu(I), contoured at 8σ, is in green. M573, M623 and M672 are shown as sticks. (*d*) The Ag(I) binding site. The bound Ag(I) is shown as a grey sphere. Anomalous map of the bound Ag(I), contoured at 10σ, is in red.

4. CRYSTAL STRUCTURES OF THE CusA–Cu(I) AND CusA–Ag(I) COMPLEXES

Intriguingly, the overall structure of the CusA–Cu(I) complex (pdb code: 3KSS) [37] is quite distinct from that of apo-CusA (figure 2). Superimposition of these two structures gives an overall r.m.s.d. of 3.9 Å (for 1006 C^{α} atoms). We used the copper edge wavelength (1.3779 Å) to collect the X-ray diffraction data of the CusA–Cu(I) crystal, thus allowing us to identify the location of the bound Cu(I). As mentioned above, the bound Cu(I) ion was found to coordinate residues M573, M623 and M672. These three methionines specifically form a typical three-methionine coordination site for binding Cu(I)/Ag(I) [43,44]. Binding of Cu(I) initiates significant conformational changes in the periplasmic as well as transmembrane domains of CusA. Perhaps the most noticeable difference between the apo and ion-bound structures appears in the PC2 region (figure 2*a*). Cu(I) binding leads to a 30° swing of the entire PC2 sub-domain. This motion shifts PC2 away from the PC1 sub-domain. The hinge for this rotational movement appears to be at the junction between sub-domains PC2 and DC, with residues G721 and P810 forming the hinge. As a consequence, the gap between PC1 and PC2 appears to open up after binding this metal ion (figure 2*b*). This gap presumably creates an entrance for metal ions from the periplasmic space. The horizontal helix, residues 665–675, located inside the cleft also makes a substantial movement. The C-terminal end of this helix is found to tilt upward by 21° in the Cu(I)-bound structure with respect to the apo form (figure 2*c*). This tilting motion allows M672 to move closer to M573 and M623 to complete the three-methionine coordination site. Coupled with this movement, TM8 also shifts in position to a more vertical orientation while retaining its α-helical structure. Overall, the N-terminal end of TM8 is found to shift away from the core by 10 Å after Cu(I) binding.

For the CusA–Ag(I) complex (pdb code: 3KSO) [37], an anomalous difference Fourier peak was found at the centre of residues M573, M623 and M672, indicating that the bound Ag^{+} ion is coordinated by these three methionines (figure 2*d*). The overall conformational changes triggered by Cu(I) and by Ag(I) binding are nearly identical. Superimposition of the CusA–Cu(I) and CusA–Ag(I) structures gives an overall r.m.s.d. of 1.0 Å (for 1021 C^{α}s). Based on the crystal structures, the horizontal helix in the cleft directly interacts with the N-terminal end of TM8. The movement of TM8 may relate directly to transmembrane signalling and could initiate the translocation of a proton across the membrane. Indeed, in the AcrB pump, there is evidence that proton translocation is coupled to the conformational change in TM8 [13,15]. The change in conformation takes place in TM8 by reeling in some random coil residues

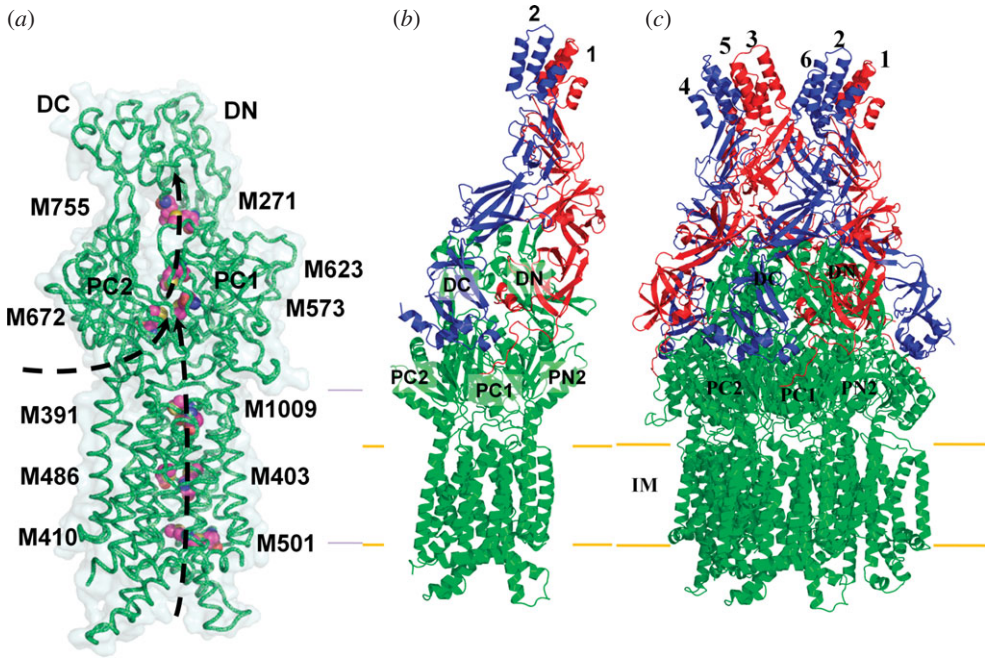

Figure 3. The methionine-residue ion relay network and the co-crystal structure of the CusBA adaptor–transporter efflux complex. (*a*) The proposed metal transport pathway of the CusA efflux pump. The five methionine pairs/clusters of the apo-CusA transporter form a pathway for metal export. These five methionines are shown as spheres (C, magenta; O, red; N, blue; S, orange). The pair M271–M755 is located at the bottom of the periplasmic funnel where the metal ion could then be released for final extrusion. The paths for metal transport through the periplasmic cleft and transmembrane region are illustrated with black curves. (*b*) Ribbon diagram of the structures of one CusA protomer (green) and two CusB protomers (red and blue) in the asymmetric unit of the crystal lattice. (*c*) Side view of the CusBA efflux complex. Each subunit of CusA is coloured green. Molecules 1, 3 and 5 of CusB are coloured red. Molecules 2, 4 and 6 of CusB are in blue.

to extend the α-helix [13]. In addition, when individual residues of the proton-relay network are changed to alanine, disrupting the hydrogen bonds in the system, it is reported that TM8 of AcrB becomes longer and extends into the periplasmic domain [15]. In contrast to AcrB, the helical structure of the N-terminus of TM8 in CusA is retained after metal binding. Instead, the N-terminal end of TM8 moves outward, together with the movement of the PC2 sub-domain.

It appears that the binding of Cu(I) or Ag(I) also triggers significant conformational changes in the other transmembrane helices of the pump. In addition to the movement of TM8, all other transmembrane helices except TM2 shift horizontally by as much as 4 Å, mimicking the motion of TM8. Further, TM1, TM3 and TM6 readjust in an approximately 3 Å upward shift with respect to the inner membrane surface. The net result is that all three of these transmembrane helices move towards the periplasm by one turn. Mutagenesis studies of the transmembrane domain of CusA indicated the conserved charged residue D405 of TM4 to be essential for transporter function [26]. Based on the crystal structure, this acidic residue interacts with E939 and K984 [37]. It is possible that these three charged residues participate in forming the proton-relay network in the transmembrane region of the pump.

Coupled with the above conformational changes, the sub-domain PN1 at the periplasmic domain was also found to undergo substantial movement. Overall, PN1 also shifts upward by 3 Å. This moves the central pore helix upward by one turn upon metal binding. It should be noted that the binding of metal ions does not significantly affect the conformation of the sub-domains DN, DC, PN2 or the transmembrane helix TM2.

5. THE METHIONINE-RESIDUE ION RELAY NETWORK

The full-length CusA includes 34 methionine residues, with 18 of them located in the transmembrane domain. Of the 18 methionines, six are paired up to form three distinct methionine pairs. These methionine pairs are M410 of TM4 and M501 of TM6; M403 of TM4 and M486 of TM6; and M391 of TM4 and M1009 of TM12 (figure 3*a*). It is known that copper tolerance proteins, such as CusF [27,28], CueR [45] and Atx1 [46], frequently use two-methionine or two-cysteine binding pockets to carry their Cu(I)/Ag(I) cargos. Thus, these methionine pairs could potentially form binding sites for Ag(I) and Cu(I) in the transmembrane region of the pump. If this is the case, then CusA could transport these metal ions from the cytoplasm along these methionine pairs. In the periplasmic domain of CusA, we have found another methionine pair (M271–M755) in addition to the three-methionine metal binding site (figure 3*a*). In view of the crystal structures, these five methionine pairs/clusters are deemed to be important for binding and transport of metal ions.

We then found that each protomer of apo-CusA forms a channel spanning the entire transmembrane region up to the bottom of the periplasmic funnel. A similar channel has also be seen in the CusA–Cu(I) structure. Intriguingly, the channel includes four methionine pairs, three (M410–M501, M403–M486

Table 1. MICs of copper and silver for different CusA mutants expressed in *E. coli* BL21(DE3)Δ*cueO*Δ*cusA*.

gene in BL21(DE3)Δ*cueO*Δ*cusA*	MIC (mM) of $CuSO_4$	MIC (μM) of $AgNO_3$
empty vector	0.50	10.0
cusA (wild-type)	2.25	30.0
cusA (M573I)	0.50	12.5
cusA (M623I)	0.50	12.5
cusA (M672I)	0.50	12.5
cusA (M391I)	1.25	10.0
cusA (M410I)	1.75	17.5
cusA (M486I)	1.75	17.5
cusA (M755I)	1.75	12.5
cusA (D405A)	0.50	12.5
cusA (E939A)	0.50	12.5
cusA (K984A)	0.50	12.5
cusA (E412A)	1.00[a]	12.5[a]
cusA (S453A)	1.00[a]	15.0[a]
cusA (C353A)	2.25[b]	
cusA (C375A)	2.25[b]	

[a]Residues E412 and S453, located in the vicinity of the triad formed by D405, E939 and K984, may also be involved in the proton-relay network.
[b]The CusA pump contains only two cysteine residues, C353 and C375, which may not be involved in copper resistance.

and M391–M1009) from the transmembrane region and one (M271–M755) from the periplasmic domain, as well as the three-methionine binding site formed by M573, M623 and M672. Taken together these five methionine pairs/clusters are likely to form a relay network facilitating metal ion transport. Remarkably, this channel spans almost the entire length of each protomer, from the transmembrane domain through to the bottom of the periplasmic funnel region, and is likely to represent a real path for transporting the metal ion from both the cytoplasm and periplasm to the periplasmic funnel for extrusion.

6. *IN VIVO* METAL SUSCEPTIBILITY ASSAY

We made an *E. coli* knocked-out strain BL21(DE3) Δ*cueO*Δ*cusA* that lacks both the *cueO* and *cusA* genes. The *cueO* gene encodes a putative multi-copper oxidase, CueO, which is also involved in copper homeostasis [47]. We mutated M573, M623 and M672, which are members of the binding site triad inside the cleft of the periplasmic domain, into isoleucines (M573I, M623I and M672I). We then expressed these three mutant transporters in BL21(DE3)Δ*cueO*Δ*cusA*, and tested their ability to confer copper and silver resistance *in vivo*. We found that the CusA mutants, M573I, M623I and M672I are unable to relieve the copper or silver sensitivity of strain BL21(DE3)Δ*cueO*Δ*cusA* (table 1), thus agreeing well with the work of Franke *et al.* [26] in which M573, M623 and M672 were shown to be essential for the function of CusA.

We mutated M410 into an isoleucine (M410I) to disrupt the pair formed by M410 and M501 at the bottom of the transmembrane and also replaced M486 and M391, which pair with M403 and M1009, with isoleucines (M486I and M391I). Expression of these three mutants in BL21(DE3)Δ*cueO*Δ*cusA* showed a significant decrease in the level of copper and silver tolerances when compared with cells expressing wild-type CusA. In addition, we introduced M755I in the periplasmic domain. Again, when expressed in BL21 (DE3)Δ*cueO*Δ*cusA*, this mutant transporter (M755I) showed a decrease in copper/silver tolerance in comparison with cells harbouring the wild-type transporter (table 1). Together, these results strongly support the hypothesis that these methionine pairs/clusters engage in the methionine-residue ion relay channel.

Based on the crystal structure of CusA, it is expected that the charged residues D405, E939 and K984 are important for the proton-relay network of the pump, and these in turn were replaced with alanines (D405A, E939A and K984A) to disrupt the hydrogen-bonded network. Indeed, cells expressing this mutant were unable to tolerate copper and silver (table 1), demonstrating that these three charged residues are essential for the transporter's functioning.

7. *IN VITRO* METAL TRANSPORT ASSAY

To investigate whether CusA can transport metal ions from the cytoplasm, we reconstituted the purified CusA protein into liposomes containing the fluorescent indicator Phen Green SK in the intravesicular space. The intravesicular and extravesicular pHs of these proteoliposomes were 6.6 and 7.0, respectively. We then determined whether these proteoliposomes can capture metal ions from the extravesicular medium with a stopped-flow transport assay. When Ag^+ ions were added into the extravesicular medium, we detected the quenching of the fluorescence signal, suggesting the uptake of Ag^+ into the intravesicular space. The uptake into proteoliposomes is presumably due to the CusA active transport activity.

In addition to the above experiment, we investigated the methionine residues that were shown to be important for copper and silver tolerances with the above transport assay. We expressed, purified and reconstituted the CusA mutants M573I, M623I and M672I into liposomes encapsulated with the same fluorescence indicator. As expected, these mutant transporters do not take up Ag^+ from the extravesicular medium of the proteoliposomes [37]. It is clear that even single point mutations M573I, M623I or M672I abolish the process of metal transport across the membrane. Thus, it is expected that this three-methionine site is requisite for both metal binding and export.

We then purified the mutants, M391I, M486I and M755I, and reconstituted them into liposomes. In these three cases, the fluorescence signals did not attenuate as indicated by the stopped-flow assay. When compared with the result from the wild-type CusA, this suggests that the M391I, M486I and M755I mutant transporters are unable to actively transport Ag^+ across the membrane. Our collective experiments provide direct compelling evidence that CusA is capable of taking up Ag^+ from the cytoplasm [37].

The crystal structure of CusA suggests that the charged residues D405, E939 and K984 in the transmembrane domain may be important for proton translocation. When reconstituted into liposomes, mutant transporters (D405A, E939A and K984A) do

not take up Ag^+ into the intravesicular space, thus confirming the importance of D405, E939 and K984 for the function of the pump [37]. This proton-relay network, formed by residues D405, E939 and K984, has to couple with the methionine-relay network upon metal-ion extrusion.

8. DYNAMICS SIMULATIONS

It is likely that CusA operates through an alternating-access mechanism [11–13]. We calculated the dynamics of the trimeric CusA pump using the elastic network model [48]. The result indeed suggests that CusA functions through three coupled motions in which the periplasmic cleft formed by sub-domains PC1 and PC2, presumably acting as the periplasmic metal entry site, alternately opens and closes.

9. CO-CRYSTAL STRUCTURE OF THE CusBA ADAPTOR–TRANSPORTER COMPLEX

The co-crystal structure of CusBA was determined to a resolution of 2.90 Å, and with the final structure includes 93 per cent of the total amino acids (pdb code: 3NE5) [38]. The structure suggests that each protomer of CusA specifically interacts with two elongated molecules of CusB (molecules 1 and 2) at the upper half portion of the periplasmic domain (figure 3*b*). The two CusB adaptors are tilted at an angle of approximately 50° with respect to the membrane surface, and establish a close fit with the transporter at the concave surface formed by domains 1 and 2 of the adaptor. It is found that molecule 1 of CusB contacts mainly the upper regions of PN2 and PC1, and the DN sub-domain of CusA. Molecule 2 of CusB, however, predominantly bridges to the upper regions of PC1 and PC2, and also the sub-domain DC of the pump. These two adaptor molecules are also seen to specifically contact one another, primarily through domains 1, 2 and 3 of these two elongated molecules. The trimeric CusA pump therefore directly contacts six CusB adaptor molecules, which form a channel at the top of the CusA trimer (figure 3*c*).

The overall conformation of the CusA protomer in the complex resembles the apo-CusA structure [37]. Superimposition of these two structures results in an r.m.s.d. of only 1.0 Å for 1019 C^α atoms. For the CusB protomers, two distinct conformations of this adaptor are captured in the complex. When we superimpose these two elongated protein structures a high r.m.s.d. of 7.5 Å is observed for the 321 C^α atoms, suggesting that the conformations of these two protomers are quite different. Interestingly, a comparison of these two molecules with the two previously determined structures of CusB [36] indicates that the four molecules display four distinct conformations, presumably representing different transient states of this MFP (figure 4*a*). This observation is consistent with the previous finding that these MFPs are highly flexible [32,35,36], with the ability to change their conformations upon ligand binding [40,42]. Indeed, it has been demonstrated that binding of metal ions trigger significant conformational changes in the CusB [42] and ZneB [40] adaptor proteins.

Previously, it was found that the N- and C-terminal ends (residues 29–88 and 386–407) of the CusB adaptor are intrinsically disordered and cannot be identified in the electron density maps of the CusB crystals [36]. Here, the co-crystal structure suggests that this region forms several short α-helices. In molecule 1 of CusB, residues 392–399 at the C-terminal end form a short α-helix. However, residues 79–95 of the N-terminus feature a long random coil and these amino acids are located immediately outside the cleft formed between sub-domains PC1 and PC2 of the CusA pump. For molecule 2 of CusB, the N-terminal residues 79–85 and 86–92 participate to form a random coil and a short α-helix, respectively. However, the C-terminal residues 382–392 and 394–400 appear to create two short α-helices. Like molecule 1 of CusB, the N-terminus of molecule 2 of CusB is near the periplasmic cleft of the pump (figure 3*c*).

It has been proposed that the N-terminal residues M49, M64 and M66 of CusB form a three-methionine metal-binding site [42]. Although these three-methionine residues cannot be identified in the electron density maps of our co-crystal, the co-crystal structure does show that the N-terminal tails of both molecules 1 and 2 of the CusB adaptors are located outside the cleft formed between PC1 and PC2 of the CusA pump. On the basis of this structure, it is possible that CusB might help to transfer the metal ions via the N-terminal three-methionine binding site into the periplasmic cleft of CusA.

10. CusA AND CusB INTERACTIONS

Intriguingly, molecule 1 of CusB interacts predominantly with CusA through charge–charge interactions. Residues K95, D386, E388 and R397 of this CusB molecule form four salt bridges with D155, R771, R777 and E584 of CusA, respectively. In addition, T89, the backbone oxygen of N91, and R292 of molecule 1 of CusB form hydrogen bonds with K594, R147, and the backbone oxygen of Q198 of CusA to secure the interaction [38]. However, the interaction between molecule 2 of CusB and CusA appears to be governed principally by charge–dipole and dipole–dipole interactions. Specifically, Q108, S109, S253 and N312 of CusB (molecule 2) form hydrogen bonds with Q785, Q194, D800 and Q198 of CusA, respectively. The backbone oxygens of L92 and T335 of this CusB molecule also contribute two additional hydrogen bonds with the side chains of K591 and T808 of the CusA pump to anchor the proteins [38].

11. CusB AND CusB INTERACTIONS

For CusB–CusB interactions, it appears that molecule 1 of CusB makes a close contact with molecule 2 of CusB. Domains 1–3 of these two molecules are involved in the binding. Residues E118, Y119, R186, E252 and R292 of molecule 1 of CusB participate to form hydrogen bonds with residues T139, D142, T206, N312 and N113 of molecule 2 of CusB, respectively [38]. Further, molecule 1 of CusB also

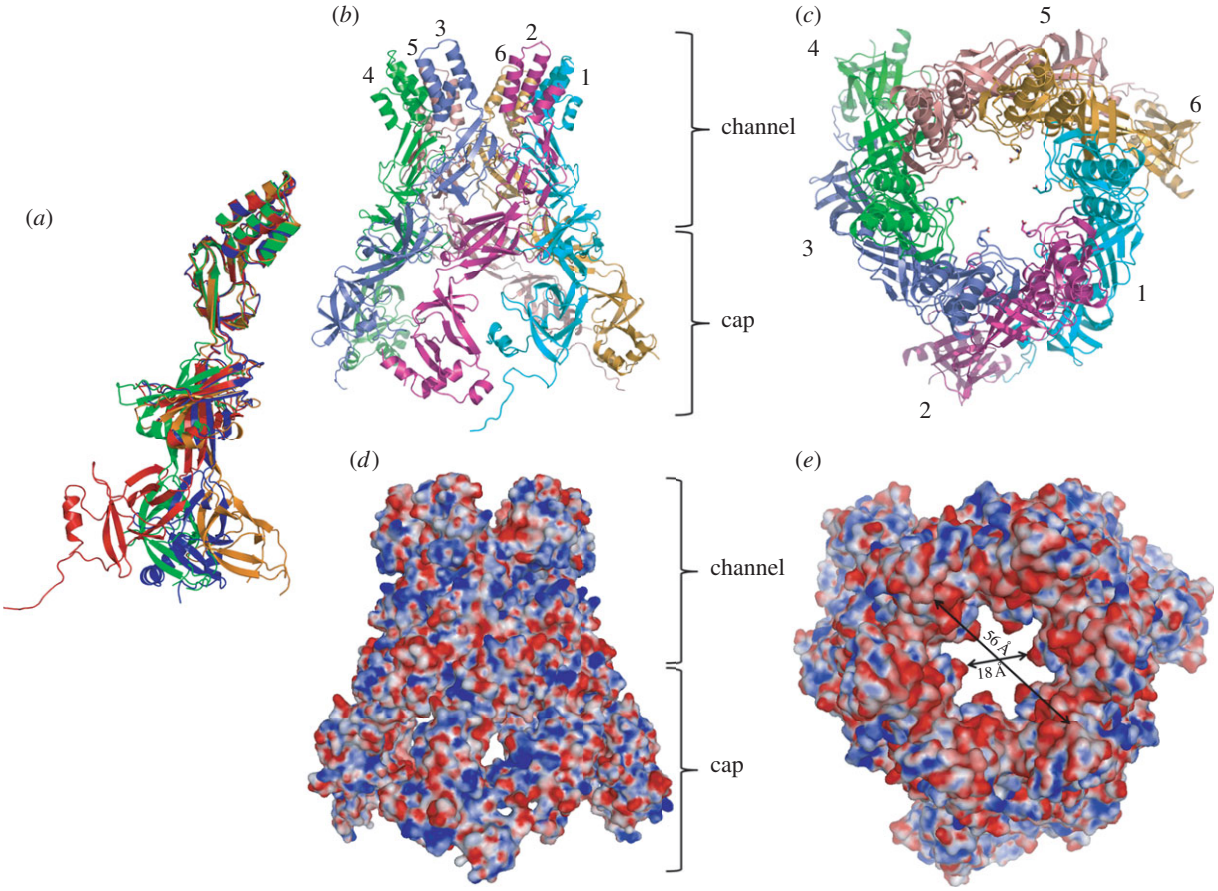

Figure 4. Comparsion of the four conformations of CusB observed in the CusBA and CusB crystals, and structure of the hexameric CusB channel. (*a*) This superimposition suggests that the main difference between the conformations of these four CusB molecules comes from domains 1 and 2 (red, molecule 1 of CusB in the CusBA co-crystal structure; blue, molecule 2 of CusB in the CusBA co-crystal structure; green, molecule A of CusB in the CusB crystal structure; orange, molecule B of CusB in the CusB crystal structure). (*b*) Side view of the hexameric CusB channel. The six molecules CusB are shown in ribbons (cyan, molecule 1; magenta, molecule 2; slate, molecule 3; green, molecule 4; pink, molecule 5; orange, molecule 6). (*c*) Top view of the hexameric CusB channel. The six molecules CusB are shown in ribbons (cyan, molecule 1; magenta, molecule 2; slate, molecule 3; green, molecule 4; pink, molecule 5; orange, molecule 6). Residue D232, which forms the narrowest region of the central channel, from each subunit of CusB is in sticks. The internal diameter of this narrowest region is approximately 18 Å. (*d*) Side view of the electrostatic surface potential of the hexameric CusB channel. This view shows the cap and channel regions formed by the CusB hexamer. Blue (+15 k_BT) and red (−15 k_BT) indicate the positively and negatively charged areas, respectively, of the protein. (*e*) Top view of the electrostatic surface potential of the hexameric CusB channel. The widest section of the hexameric channel appears to form at the top edge with its internal diameter of approximately 56 Å. Blue (+15 k_BT) and red (−15 k_BT) indicate the positively and negatively charged areas, respectively, of the protein.

contributes to contact molecule 6 of CusB, which is anchored to the next subunit of CusA. The majority of the interactions come from domains 2 and 3 of these two molecules. Particularly, residues N113, N228 and N312 of molecule 1 of CusB pair up with R292, the backbone oxygen of A126, and E252 of molecule 6 of CusB to form three hydrogen bonds. In addition, D142 of molecule 1 of CusB participates to form two hydrogen bonds with Y119 and R297 of molecule 6 of CusB to secure the binding [38].

12. THE HEXAMERIC CusB CHANNEL

The co-crystal structure suggests that CusB forms a hexamer above the trimeric CusA pump (figure 4*b*,*c*). This hexameric arrangement allows the MFPs to create a funnel-like structure with the central channel formed along the crystallographic threefold symmetry axis. Six of these CusB protomers use a side-by-side fashion to pack against one another to form this funnel (figure 4*b*). In view of the structure, it appears that domain 1 and the lower half of domain 2 of CusB primarily create a cap-like structure, whereas the upper half of domain 2, domain 3 and domain 4 of the adaptor contribute to the central channel of the funnel (figure 4*b*,*d*). The inner surface of the cap fits closely with the outer surface of the upper portion of the periplasmic domain of the CusA trimer. The channel formed above the cap of the adaptor is approximately 62 Å long with an average internal diameter of approximately 37 Å. Thus, the interior of the channel gives rise to a large elongated cavity with a volume of approximately 65 000 Å^3. The lower half of the channel is primarily created by β-barrels, whereas the upper half is an all α-helical tunnel. Presumably, this channel is filled with solvent molecules. The diameter of the channel is gradually constricted and then dilated as it approaches the outer membrane. Thus, the α-helices of domain 4 create an inverted conical structure. The narrowest section of the central channel is located at

residue D232, which is close to the hinge region between domains 3 and 4 of the MFP (figure 4*c*). The widest section of the channel appears to form at 56 Å. The inner surface of the channel is predominantly negatively charged, as indicated by the electrostatic surface diagram (figure 4*e*), which suggests that the interior surface of the channel may have the capacity to bind positively charged metal ions.

The co-crystal structure presented here highlights the structural importance of the periplasmic MFP. Given the fact that six CusB molecules assemble to form a channel at the CusA funnel top, this suggests that the adaptor is likely to be involved in the active efflux of metal ions. The hexameric arrangement of these MFPs has also been observed in the crystal structure of MacA in which six protomers assemble to create a large channel [39]. Thus, in addition to their role as adaptors to bridge the inner and outer membrane efflux components, we can anticipate that these MFPs are likely to actively participate in extrusion of their substrates.

13. ISOTHERMAL TITRATION CALORIMETRY FOR CusA AND CusB BINDING

We used isothermal titration calorimetry (ITC) to determine the binding affinity of CusB to the CusA pump. The ITC data indicate an equilibrium dissociation constant of 5.1 ± 0.3 μM [38]. The titration is characterized by a negative enthalpic contribution ($\Delta H = -22.4 \pm 0.3$ kcal mol^{-1}), which yields a hyperbolic binding curve. The entropic contribution (ΔS) of this binding reaction was found to be -50.9 cal mol^{-1} deg^{-1}. Interestingly, the molecular ratio for this binding reaction based on ITC is one CusA monomer per two CusB protomers [38]. This result is indeed confirmed by the crystal structure where each protomer of CusA binds two molecules of CusB.

Recently, artificial peptides, DARPins, have been introduced to bind and effectively inhibit the AcrB transporter [13]. The inhibitor-binding site is found right above the cleft formed between PC1 and PC2 of AcrB [13]. Interestingly, the location of this inhibitor-binding site corresponds to the binding site for molecule 2 of CusB in the CusBA complex. Thus, it is likely that the mechanism of action for these inhibitors may be the disruption of the adaptor–transporter interaction by competition. If this is the case, then a proposed $AcrB_3$–$AcrA_3$–$TolC_3$ model [35] containing only one protomer of AcrA per AcrB protomer would not be sufficient to form a functional pump. Indeed, it has been recently demonstrated that AcrA and AcrB interact with the stoichiometry of 2 : 1 adaptor-to-transporter molar ratio [49].

14. DOCKING OF CusC ONTO CBA

Recently, the crystal structure of the CusC channel has been determined [50]. The structure suggests that this channel protein resembles the architectures of the OprM [31] and TolC [30] channels. To understand how the CusBA complex interacts with CusC, we constructed a CusCBA fitting model based on the crystal structures of CusBA [38] and CusC [50]. A steered molecular dynamics simulation was used to rigidly dock the trimeric CusC channel to the crystal form of the hexameric CusB channel bound to the trimeric CusA pump. During the rigid-body docking process, the molecules were aligned with the *z*-axis (the three-fold symmetry axis). CusB was then held rigidly, allowing CusC to pull along the *z*-axis towards CusB until no further change in the centre of mass was measured. As the inner diameter of the top portion of the hexameric CusB channel is larger than the outer diameter of the periplasmic end of the trimeric CusC channel, this suggests that the CusC channel could easily be inserted into the CusB channel when they contact one another. After optimizing this docked model, the final structure of the CusCBA complex suggests that CusC interacts with CusBA at the interior of the upper half of the channel formed by the α-helical domain (domain 4) of CusB, primarily through coiled-coil interaction (figure 5*a*).

Genetic experiments revealed that the α-helical domain of the TolC channel is mapped predominantly to the β-barrel domain of the AcrA adaptor [51]. This result has led to the hypothesis that the MexA adaptor provides two binding sites for the periplasmic α-helices of the OprM channel, one at the α-hairpin domain and the other at the β-barrel domain [34]. These two domains should correspond to domain 4 and domain 2 of CusB, respectively. It is likely that the above docked CusCBA structure is a useful snapshot for how CusBA recruits CusC at the early stage. To pump metal ions, the CusC channel may need to contact the top of CusA. Interestingly, the CusBA crystal structure suggests that the funnel top of the trimeric CusA pump is surrounded with domain 2 of the CusB hexamer. Thus, it is likely that the funnel top of CusA, α-helical end of CusC, and domain 2 of CusB may contact one another during the extrusion cycle (figure 5*b*). If this is the case, then it is possible that the recruitment of the CusC channel to the tripartite complex is a two-stage process. The first step may involve an interaction between both the α-helical domains of CusB and CusC. Then, the CusC channel could slide further down the CusB channel and contact the top of CusA, whereas this region is surrounded with domain 2 of the CusB hexamer (figure 5).

We thus investigated the possible interaction of CusC with domain 2 of CusB, which also brings it into close proximity to CusA. First, the trimeric CusA pump and domains 1 and 2 of the hexameric CusB channel were held rigidly, while domains 3 and 4 of each CusB monomer were pulled outward using customized harmonic forces to open the annulus of the hexameric channel. Next, we manually inserted CusC into the opened CusB ring. Finally, simulated annealing followed by energy minimization was performed to relax CusB and CusC from these positions and allow them to assume a lower energy conformation (figure 5*b*). All simulations were performed using nanoscale molecular dynamics (NAMD) [52] and the chemistry at Harvard macromolecular mechanics 27 (CHARMM27) with a phi–psi cross term map correction (CMAP) force field [53]. The final $CusC_3$–$CusB_6$–$CusA_3$ structural models represent a 750 kDa tripartite efflux complex spanning both the inner and outer membranes of *E. coli* to extrude Cu(I)/Ag(I) (figure 5).

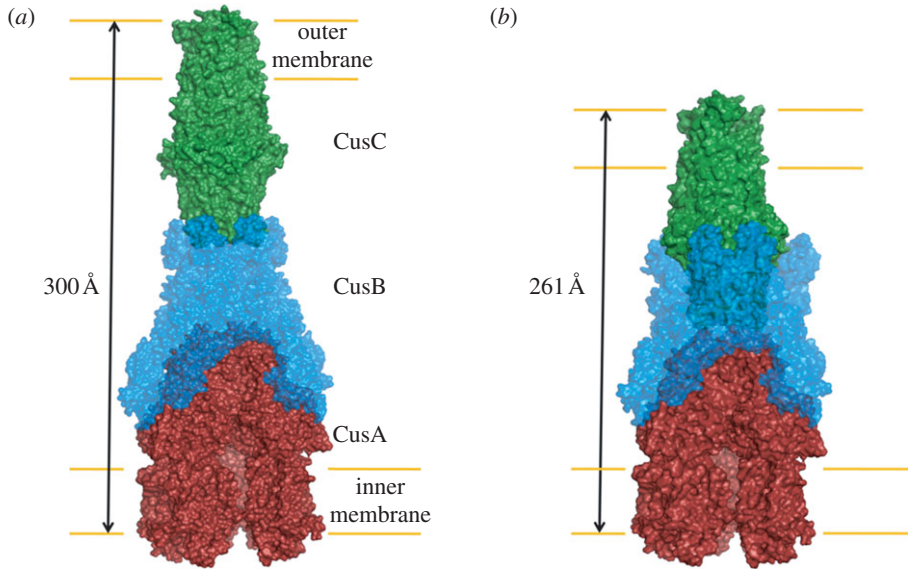

Figure 5. Docking of CusC to CusBA. (*a*) The α-helical end of CusC interacts with the α-helices (domain 4) of CusB in the CusBA complex. (*b*) The funnel top of CusA, α-helical end of CusC and domain 2 of CusB contact one another when the CusC channel slides further down the hexameric CusB channel. The surface rendering of the $CusC_3$–$CusB_6$–$CusA_3$ complex is coloured as follows: green, CusC trimer; blue, CusB hexamer; red, CusA trimer.

15. PROPOSED MECHANISM FOR METAL-ION EXPORT

We believe that CusA can pick up metal ions from both the cytoplasm and periplasm. A similar suggestion has been made for the CzcA [54] and AcrD [18] efflux pumps. However, the major path for ion efflux should be carried out through the periplasm [55]. We propose that the CusA transporter uses methionine pairs/clusters to export Cu(I) and Ag(I). The periplasmic cleft of CusA presumably remains closed when there is no Cu(I)/Ag(I). In the presence of Cu(I) or Ag(I) ions, the periplasmic cleft opens. Metal ions could enter the three-methionine binding site, formed by M573, M623 and M672, inside the cleft between sub-domains PN2 and PC1 on the periplasmic portion of CusA or via the methionine pairs within the transmembrane domain of the pump. It has been demonstrated that the chaperone CusF can directly transfer its bound Cu(I) to the CusB MFP [56]. Thus, it is likely that CusF is responsible for delivering metal ions to the CusCBA tripartite efflux system in the periplasm. There is a chance that the initial step of metal transport through the periplasmic cleft of the CusA pump may involve a direct transfer from CusF to the previously proposed three-methionine metal binding site [42] (M49, M64 and M66) at the long N-terminal tail of CusB. Based on the co-crystal structure of CusBA, each flexible tail of CusB is located near the PN2/PC1 cleft of the CusA pump. Thus, the second step could well be a delivering of the bound metal ion from CusB to the three-methionine cluster (M573, M623 and M672) inside the periplasmic cleft of CusA [37]. The bound metal ion could then be released to the nearest methionine pair (M271–M755) located directly above the three-methionine metal binding site [37], from which the ion could be released into the central funnel of CusA and eventually the CusC channel for final extrusion. It is not yet known whether the interior of the hexameric CusB channel forms part of the extrusion pathway for Cu(I) and Ag(I). Based on the crystal structures of CusBA [38] and CusC [50], the interior surface of both the hexameric CusB and trimeric CusC channels are predominantly negatively charged and the interior surface of CusC is more electronegative. Thus, it is likely that the last step of transport of cationic Cu(I) and Ag(I) is facilitated by the negative potential gradient created by the CusB and CusC channels. During metal-ion extrusion, a large conformational change of CusC may occur to open this OMC, similar to the cases of TolC [57] and OprM [58]. Exactly what this tripartite efflux system's mechanism is must await confirmation by elucidation of additional crystal structures of the CusCBA tripartite complex.

16. CONCLUDING REMARKS

It is clear from the published literature that the RND efflux pumps have significant functions in conferring resistance to clinically relevant antimicrobials [59]. Thus, it is very important to understand how these tripartite pumps work and assemble. To date, a crystallographic model of these tripartite efflux complexes has not been reported. One direct approach to obtain the complete picture of these efflux complexes is to elucidate the structures of individual components as well as the assembled complexes of these efflux systems. This approach should allow us rationally to design inhibitors that prohibit different components of the pumps assembling, thus preventing these pumps from functioning. In the case of the Cus efflux system, the availability of the co-crystal structures of the adaptor–transporter CusBA, the channel-adaptor CusCB, and the complete tripartite CusCBA efflux complexes are essential in order to achieve this task, although co-crystallization of different components of these RND efflux systems has proven to be extremely difficult.

This work is supported by an NIH Grant R01GM086431 (E.W.Y.).

REFERENCES

1 Silver, S. 2003 Bacterial silver resistance: molecular biology and uses and misuses of silver compounds. *FEMS Microbiol. Rev.* **27**, 341–353. (doi:10.1016/S0168-6445(03)00047-0)

2 Percival, S. L., Bowler, P. G. & Russell, D. 2005 Bacterial resistance to silver in wound care. *J. Hosp. Infect.* **60**, 1–7. (doi:10.1016/j.jhin.2004.11.014)

3 Ercal, N., Gurer-Orhan, H. & Aykin-Burns, N. 2001 Toxic metals and oxidative stress part I: mechanisms involved in metal induced oxidative damage. *Curr. Topics Med. Chem.* **1**, 529–539. (doi:10.2174/1568026013394831)

4 Tseng, T. T., Gratwick, K. S., Kollman, J., Park, D., Nies, D. H., Goffeau, A. & Saier Jr, M. H. 1999 The RND permease superfamily: an ancient, ubiquitous and diverse family that includes human disease and development protein. *J. Mol. Microbiol. Biotechnol.* **1**, 107–125.

5 Nies, D. H. 2003 Efflux-mediated heavy metal resistance in prokaryotes. *FEMS Microbiol. Rev.* **27**, 313–339. (doi:10.1016/S0168-6445(03)00048-2)

6 Zgurskaya, H. & Nikaido, H. 1999 Bypassing the periplasm: reconstitution of the AcrAB multidrug efflux pump of *Escherichia coli*. *Proc. Natl Acad. Sci. USA* **96**, 7190–7195. (doi:10.1073/pnas.96.13.7190)

7 Nishino, K. & Yamaguchi, A. 2001 Analysis of a complete library of putative drug transporter genes in *Escherichia coli*. *J. Bacteriol.* **183**, 5803–5812. (doi:10.1128/JB.183.20.5803-5812.2001)

8 Murakami, S., Nakashima, R., Yamashita, E. & Yamaguchi, A. 2002 Crystal structure of bacterial multidrug efflux transporter AcrB. *Nature* **419**, 587–593. (doi:10.1038/nature01050)

9 Yu, E. W., McDermott, G., Zgruskaya, H. I., Nikaido, H. & Koshland Jr, D. E. 2003 Structural basis of multiple drug binding capacity of the AcrB multidrug efflux pump. *Science* **300**, 976–980. (doi:10.1126/science.1083137)

10 Yu, E. W., Aires, J. R., McDermott, G. & Nikaido, H. 2005 A periplasmic drug-binding site of the AcrB multidrug efflux pump: a crystallographic and site-directed mutagenesis study. *J. Bacteriol.* **187**, 6804–6815. (doi:10.1128/JB.187.19.6804-6815.2005)

11 Murakami, S., Nakashima, R., Yamashita, E., Matsumoto, T. & Yamaguchi, A. 2006 Crystal structures of a multidrug transporter reveal a functionally rotating mechanism. *Nature* **443**, 173–179. (doi:10.1038/nature05076)

12 Seeger, M. A., Schiefner, A., Eicher, T., Verrey, F., Dietrichs, K. & Pos, K. M. 2006 Structural asymmetry of AcrB trimer suggests a peristaltic pump mechanism. *Science* **313**, 1295–1298. (doi:10.1126/science.1131542)

13 Sennhauser, G., Amstutz, P., Briand, C., Storchengegger, O. & Grütter, M. G. 2007 Drug export pathway of multidrug exporter AcrB revealed by DARPin inhibitors. *PLoS Biol.* **5**, e7. (doi:10.1371/journal.pbio.0050007)

14 Das, D., Xu, Q. S., Lee, J. Y., Ankoudinova, I., Huang, C., Lou, Y., Degiovanni, A., Kim, R. & Kim, S. H. 2007 Crystal structure of the multidrug efflux transporter AcrB at 3.1 Å resolution reveals the N-terminal region with conserved amino acids. *J. Struct. Biol.* **158**, 494–502. (doi:10.1016/j.jsb.2006.12.004)

15 Su, C.-C., Li, M., Gu, R., Takatsuka, Y., McDermott, G., Nikaido, H. & Yu, E. W. 2006 Conformation of the AcrB multidrug efflux pump in mutants of the putative proton relay pathway. *J. Bacteriol.* **188**, 7290–7296. (doi:10.1128/JB.00684-06)

16 Törnroth-Horsefield, S., Gourdon, P., Horsefield, R., Brive, L., Yamamoto, N., Mori, H., Snijder, A. & Neutze, R. 2007 Crystal structure of AcrB in complex with a single transmembrane subunit reveals another twist. *Structure* **15**, 1663–1673. (doi:10.1016/j.str.2007.09.023)

17 Rosenberg, E. Y., Ma, D. & Nikaido, H. 2000 AcrD of *Escherichia coli* is an aminoglycoside efflux pump. *J. Bacteriol.* **182**, 1754–1756. (doi:10.1128/JB.182.6.1754-1756.2000)

18 Aires, J. R. & Nikaido, H. 2005 Aminoglycosides are captured from both periplasm and cytoplasm by the AcrD multidrug efflux transporter of *Escherichia coli*. *J. Bacteriol.* **187**, 1923–1929. (doi:10.1128/JB.187.6.1923-1929.2005)

19 Ma, D., Cook, D. N., Alberti, M., Pon, N. G., Nikaido, H. & Hearst, E. 1993 Molecular cloning of *acrA* and *acrE* genes of *Escherichia coli*. *J. Bacteriol.* **175**, 6299–6313.

20 Lau, S. Y. & Zgurskaya, H. I. 2005 Cell division defects in *Escherichia coli* deficient in the multidrug efflux transporter AcrEF-TolC. *J. Bacteriol.* **187**, 7815–7825. (doi:10.1128/JB.187.22.7815-7825.2005)

21 Baranova, N. & Nikaido, H. 2002 The BaeSR two-component regulatory system activates transcription of *yegMNOB* (*mdtABCD*) transporter gene cluster in *Escherichia coli* and increases its resistance to novobiocin and deoxycholate. *J. Bacteriol.* **184**, 4168–4176. (doi:10.1128/JB.184.15.4168-4176.2002)

22 Nagakubo, S., Nishino, K., Hirata, T. & Yamaguchi, A. 2002 The putative response regulator BaeR stimulates multidrug resistance of *Escherichia coli* via a novel multidrug exporter system, MdtABC. *J. Bacteriol.* **184**, 4161–4167. (doi:10.1128/JB.184.15.4161-4167.2002)

23 Bohnert, J. A., Schuster, S., Fähnrich, E., Trittler, R. & Kern, W. V. 2007 Altered spectrum of multidrug resistance associated with a single point mutation in the *Escherichia coli* RND-type MDR efflux pump YhiV (MdtF). *J. Antimicrob. Chemother.* **6**, 1216–1222. (doi:10.1093/jac/dkl426)

24 Kobayashi, A., Hirakawa, H., Hirata, T., Nishino, K. & Yamaguchi, A. 2001 Growth phase-dependent expression of drug exporters in *Escherichia coli* and its contribution to drug tolerance. *J. Bacteriol.* **16**, 5693–5703.

25 Franke, S., Grass, G. & Nies, D. H. 2001 The product of the *ybdE* gene of the *Escherichia coli* chromosome is involved in detoxification of silver ions. *Microbiol.* **147**, 965–972.

26 Franke, S., Grass, G., Rensing, C. & Nies, D. H. 2003 Molecular analysis of the copper-transporting efflux system CusCFBA of *Escherichia coli*. *J. Bacteriol.* **185**, 3804–3812. (doi:10.1128/JB.185.13.3804-3812.2003)

27 Xue, Y., Davis, A. V., Balakrishnan, G., Stasser, J. P., Staehlin, B. M., Focia, P., Spiro, T. G., Penner-Hahn, J. E. & O'Halloran, T. V. 2008 Cu(I) recognition via cation-π and methionine interactions in CusF. *Nature Chem. Biol.* **4**, 107–109. (doi:10.1038/nchembio.2007.57)

28 Loftin, I. R., Franke, S., Blackburn, N. J. & McEvoy, M. M. 2007 Unusual Cu(I)/Ag(I) coordination of *Escherichia coli* CusF as revealed by atomic resolution crystallography and X-ray absorption spectroscopy. *Protein Sci.* **16**, 2287–2293. (doi:10.1110/ps.073021307)

29 Sennhauser, G., Bukowska, M. A., Briand, C. & Grütter, M. G. 2009 Crystal structure of the multidrug exporter MexB from *Pseudomonas aeruginosa*. *J. Mol. Biol.* **389**, 134–145. (doi:10.1016/j.jmb.2009.04.001)

30 Koronakis, V., Sharff, A., Koronakis, E., Luisi, B. & Hughes, C. 2000 Crystal structure of the bacterial membrane protein TolC central to multidrug efflux and

protein export. *Nature* **405**, 914–919. (doi:10.1038/35016007)
31 Akama, H., Kanemaki, M., Yoshimura, M., Tsukihara, T., Kashiwag, T., Yoneyama, H., Narita, S., Nakagawa, A. & Nakae, T. 2004 Crystal structure of the drug discharge outer membrane protein, OprM, of *Pseudomonas aeruginosa*. *J. Biol. Chem.* **279**, 52 816–52 819.
32 Mikolosko, J., Bobyk, K., Zgurskaya, H. I. & Ghosh, P. 2006 Conformational flexibility in the multidrug efflux system protein AcrA. *Structure* **14**, 577–587. (doi:10.1016/j.str.2005.11.015)
33 Higgins, M. K., Bokma, E., Koronakis, E., Hughes, C. & Koronakis, V. 2004 Structure of the periplasmic component of a bacterial drug efflux pump. *Proc. Natl Acad. Sci. USA* **101**, 9994–9999. (doi:10.1073/pnas.0400375101)
34 Akama, H., Matsuura, T., Kashiwag, S., Yoneyama, H., Narita, S., Tsukihara, T., Nakagawa, A. & Nakae, T. 2004 Crystal structure of the membrane fusion protein, MexA, of the multidrug transporter in *Pseudomonas aeruginosa*. *J. Biol. Chem.* **279**, 25 939–25 942. (doi:10.1074/jbc.C400164200)
35 Symmons, M., Bokma, E., Koronakis, E., Hughes, C. & Koronakis, V. 2009 The assembled structure of a complete tripartite bacterial multidrug efflux pump. *Proc. Natl Acad. Sci. USA* **106**, 7173–7178.
36 Su, C.-C. *et al.* 2009 Crystal structure of the membrane fusion protein CusB from *Escherichia coli*. *J. Mol. Biol.* **393**, 342–355. (doi:10.1016/j.jmb.2009.08.029)
37 Long, F., Su, C.-C., Zimmermann, M. T., Boyken, S. E., Rajashankar, K. R., Jernigan, R. L. & Yu, E. W. 2010 Crystal structures of the CusA efflux pump suggest methionine-mediated metal transport. *Nature* **467**, 484–488. (doi:10.1038/nature09395)
38 Su, C.-C., Long, F., Zimmermann, M. T., Rajashankar, K. R., Jernigan, R. L. & Yu, E. W. 2011 Crystal structure of the CusBA heavy-metal efflux complex of *Escherichia coli*. *Nature* **470**, 558–562. (doi:10.1038/nature09743)
39 Yum, S. *et al.* 2009 Crystal structure of the periplasmic component of a tripartite macrolide-specific efflux pump. *J. Mol. Biol.* **387**, 1286–1297. (doi:10.1016/j.jmb.2009.02.048)
40 De Angelis, F. *et al.* 2010 Metal-induced conformational changes in ZneB suggest an active role of membrane fusion proteins in efflux resistance systems. *Proc. Natl Acad. Sci. USA* **107**, 11 038–11 043.
41 Borges-Walmsley, M. I., Beauchamp, J., Kelly, S. M., Jumel, K., Candlish, D., Harding, S. E., Price, N. C. & Walmsley, A. R. 2003 Identification of oligomerization and drug-binding domains of the membrane fusion protein EmrA. *J. Biol. Chem.* **278**, 12 903–12 912.
42 Bagai, I., Liu, W., Rensing, C., Blackburn, N. J. & McEvoy, M. M. 2007 Substrate-linked conformational change in the periplasmic component of a Cu(I)/Ag(I) efflux system. *J. Biol. Chem.* **282**, 35 695–35 702.
43 Zhou, H. & Thiele, D. J. 2001 Identification of a novel high affinity copper transport complex in the fission yeast *Schizosaccharomyces pombe*. *J. Biol. Chem.* **276**, 20 529–20 535.
44 Jiang, J., Nadas, I. A., Kim, M. A. & Franz, K. J. 2005 A Mets motif peptide found in copper transport proteins selectively binds Cu(I) with methionine-only coordination. *Inorg. Chem.* **44**, 9787–9794. (doi:10.1021/ic051180m)
45 Changela, A., Chen, K., Xue, Y., Holschen, J., Outten, C. E., O'Halloran, T. V. & Mondragón, A. 2003 Molecular basis of metal-ion selectivity and zeptomolar sensitivity by CueR. *Science* **301**, 1383–1387. (doi:10.1126/science.1085950)
46 Arnesano, F., Banci, L., Bertini, I., Huffman, D. L. & O'Halloran, T. V. 2001 Solution structure of the Cu(I) and apo-forms of the yeast metallochaperone, Atx1. *Biochemistry* **40**, 1528–1539. (doi:10.1021/bi0014711)
47 Grass, G. & Rensing, C. 2001 Genes involved in copper homeostasis in *Escherichia coli*. *J. Bacteriol.* **183**, 2145–2147. (doi:10.1128/JB.183.6.2145-2147.2001)
48 Atilgan, A. R., Durell, S. R., Jernigan, R. L., Demirel, M. C., Keskin, O. & Bahar, I. 2001 Anisotropy of fluctuation dynamics of proteins with an elastic network model. *Biophys. J.* **80**, 505–515. (doi:10.1016/S0006-3495(01)76033-X)
49 Tikhonova, E. B., Yamada, Y. & Zgurskaya, H. I. 2011 Sequential mechanism of assembly of multidrug efflux pump AcrAB-TolC. *Chem. Biol.* **18**, 454–463. (doi:10.1016/j.chembiol.2011.02.011)
50 Kulathila, R., Kulathila, R., Indic, M. & van den Berg, B. 2011 Crystal structure of *Escherichia coli* CusC, the outer membrane component of a heavy metal efflux pump. *PLoS ONE* **6**, e15610. (doi:10.1371/journal.pone.0015610)
51 Gerken, H. & Misra, R. 2004 Genetic evidence for functional interactions between TolC and AcrA proteins of a major antibiotic efflux pump of *Escherichia coli*. *Mol. Microbiol.* **54**, 620–631. (doi:10.1111/j.1365-2958.2004.04301.x)
52 Phillips, J. C. *et al.* 2005 Scalable molecular dynamics with NAMD. *J. Comp. Chem.* **26**, 1781–1802. (doi:10.1002/jcc.20289)
53 Feller, S. E. & MacKerell Jr, A. D., 2000 An improved empirical potential energy for molecular simulations of phospholipids. *J. Phys. Chem. B* **104**, 7510–7515. (doi:10.1021/jp0007843)
54 Goldberg, M., Pribyl, T., Juhuke, S. & Nies, D. H. 1999 Energetics and topology of CzcA, a cation/proton antiporter of the resistance-nodulation-cell division protein family. *J. Biol. Chem.* **274**, 26 065–26 070.
55 Kim, E.-H., Nies, D. H., McEvoy, M. M. & Rensing, C. 2011 Switch or funnel: how RND-type transport systems control periplasmic metal homeostasis. *J. Bacteriol.* **193**, 2381–2387. (doi:10.1128/JB.01323-10)
56 Bagai, I., Rensing, C., Blackburn, N. J. & McEvoy, M. M. 2008 Direct metal transfer between periplasmic proteins identifies a bacterial copper chaperone. *Biochemistry* **47**, 11 408–11 414.
57 Vaccaro, L., Scott, K. A. & Sansom, M. S. P. 2008 Gating at both ends and breathing in the middle: conformational dynamics of TolC. *Biophys. J.* **95**, 5681–5691. (doi:10.1529/biophysj.108.136028)
58 Phan, G., Benabdelhak, H., Lascombe, M.-B., Benas, P., Rety, S., Picard, M., Ducruix, A., Etchebest, C. & Broutin, I. 2010 Structural and dynamical insights into the opening mechanism of *P. aeruginosa* OprM channel. *Structure* **18**, 507–517. (doi:10.1016/j.str.2010.01.018)
59 Piddock, L. J. V. 2006 Clinically relevant chromosomally encoded multidrug resistance efflux pumps in bacteria. *Clin. Microbiol. Rev.* **19**, 382–402. (doi:10.1128/CMR.19.2.382-402.2006)